Publications of the Korean Astronomical Society
32: 239 ∼ 244, 2017 March

pISSN 1225-1534
eISSN 2287-6936
https://doi.org/10.5303/PKAS.2017.32.1.239

AKARI-NEP : EFFECTS OF AGN PRESENCE ON SFR ESTIMATES OF GALAXIES

L. Marchetti[1], A. Feltre[2], S. Berta[3], I. Baronchelli[4], S. Serjeant[1], M. Vaccari[5], D. Bulgarella[6], M. Karouzos[7], K. Murata[8,9], N.Oi[9], C. Pearson[10,1], G. Rodighiero[4], C. Segdwick[1], and G.J. White[1,10]

[1]Department of Physical Sciences, The Open University, Milton Keynes, MK7 6AA, UK
[2]Institute d'Astrophysique de Paris
[3]Max-Planck-Institut für extraterrestrische Physik (MPE), Postfach 1312, 85741, Garching, Germany
[4]Dipartimento di Fisica e Astronomia, Università degli Studi di Padova
[5]Astrophysics Group, Physics Department, University of the Western Cape, Cape Town South Africa
[6]Aix-Marseille Université, CNRS, LAM (Laboratoire d'Astrophysique de Marseille) UMR7326, 13388, Marseille, France
[7]Department of Physics and Astronomy, Seoul National University, Gwanak-gu, Seoul 151-742, Korea
[8]Department of Space and Astronautical Science, GUAS, 753-8511, Yamaguchi, Japan
[9]Institute of Space and Astronautical Science, JAXA, Sagamihara, 252-5210, Kanagawa, Japan
[10]RAL Space, Rutherford Appleton Laboratory

E-mail: lucia.marchetti@open.ac.uk

(Received September 1, 2015; Revised October 20, 2016; Accepted October 20, 2016)

ABSTRACT

How does the presence of an AGN influence the total SFR estimates of galaxies and change their distribution with respect to the *Galaxy Main Sequence*? To contribute to solving this question, we study a sample of 1133 sources detected in the North Ecliptic Pole field (NEP) by AKARI and Herschel. We create a multi-wavelength dataset for these galaxies and we fit their multi-wavelength Spectral Energy Distribution (SED) using the whole spectral regime (from 0.1 to 500 μm). We perform the fit using three procedures: `LePhare` and two optimised codes for identifying AGN tracers from the SED analysis. In this work we present an overview of the comparison between the estimates of the Infrared bolometric luminosities (between 8 and 1000 μm) and the AGN fractions obtained exploiting these different procedures. In particular, by estimating the AGN contribution in four different wavelength ranges (5-40 μm, 10-20 μm, 20-40 μm and 8-1000 μm) we show how the presence of an AGN affects the PAH emission by suppressing the ratio $\frac{L_{8\ \mu\mathrm{m}}}{L_{4.5\ \mu\mathrm{m}}}$ as a function of the considered wavelength range.

Key words: Galaxies, AGN, Infrared

1. INTRODUCTION

Infrared space missions, such as AKARI (Murakami et al. 2007), Spitzer (Werner et al. 2004) and Herschel (Pilbratt et al. 2010) have clearly showed that the bulk of the star formation in galaxies occurs in obscured dusty regions with the peak of their emission in the IR/sub-mm regime. For this reason AKARI and Herschel together provide us with a unique dataset to study star forming galaxies across cosmic time. Thanks to their combined observations in 14 bands between 1.7 to 500 μm, together with surveys at shorter wavelengths, we are able to carefully study the panchromatic SED of IR galaxies and thus their physical properties such as the star formation (SF) and the stellar masses (M_*). Herschel allows to characterise the peak of the IR emission of galaxies up to high redshift and many studies have been conducted with this intent, but there are still many open questions that yet need to be solved, for example: do mergers and/or AGN feedback trigger and or regulate the star formation of FIR galaxies? In particular, many recent studies have been arguing the role played by AGN and BH accretion in galaxy formation and evo-

lution and how these are connected with the star formation activity in galaxies (e.g. Delvecchio et al. 2014; Elbaz et al. 2011). Starburst sources characterised by a high SFR are likely to happen simultaneously or coexist with the presence of an AGN which has been demonstrated both theoretically and by the observations (e.g., Bower et al. 2006; Farrah et al. 2003; Brusa et al. 2014) . For this reason it has become more and more important to characterise the interplay between the star formation activity and the nuclear gravitational accretion activity. Moreover, many authors have shown that exists a correlation between M_* and SFR that defines the so called *Galaxy Main Sequence* (Elbaz et al. 2011) which appears to evolve with cosmic time. How galaxies are distributed in this parameter space is still debated and e.g., **?**, have shown that many of the off-main sequence objects require the presence of an AGN to justify their properties. The aim of the present work is to contribute to address these phenomena. We can carefully study the AGN contribution to the total SFR by means of the dense sampling in wavelength provided by AKARI in the regime between 2 and 24 μm where the AGN emission contributes the most to the SED. This allows us to better distinguish between objects dominated by the starburst activity and those dominated by AGN and in which proportions these emissions contribute to the total energy distribution of these galaxies. We present here some preliminary results obtained by our analysis, while the conclusive analysis will be developed in Marchetti et al., in prep. This work is structured as follows. In Section 2 we describe our multi-wavelength dataset, the selection of the samples and the source identification. In Section 3 we describe the SED fitting procedures adopted for our analysis, while in Section 4 we report the results. In Section 5 we report a summary and some future perspective. Throughout the paper we adopt a standard cosmology with $\Omega_M = 0.3$, $\Omega_\Lambda = 0.7$, $H_0 = 70$ km s^{-1} Mpc^{-1}.

2. THE SAMPLE SELECTION

AKARI carried out both a narrow/deep and a wide/shallow surveys centred in the North Ecliptic Pole (hereafter NEP). Afterwards Herschel has observed with both PACS and SPIRE 9 deg^2 that covers both the deep and the wide AKARI surveys centred on the NEP.

For this reason we use the multi-wavelength AKARI catalogue assembled by Murata et al. (2013) in the deep survey area, which covers only the central region of the area observed with Herschel, together with the shallower collection by Kim et al. (2012) which covers a larger area than the deep one (see Oi et al. 2014 for the coverage map). These catalogues contain photometry from the optical to the AKARI *L24* filter. Oi et al. (2014) also provide the photometric redshifts for all the sources in the deep catalogue. We then add the catalogue of spectroscopic redshifts by Shim et al. (2013) and the UV GALEX photometry by Mazyed et al., in preparation. We use the Herschel source extraction developed by Mazyed et al., in preparation using `DAOPHOT`. The final multi-wavelength collection has been created by performing a positional crossmatching of the various catalogues using different search radius according to the dimension of the characteristic point spread function (*PSF*) of each survey. The final sample contains 1133 sources and is defined by a 3 σ detection threshold at any of the 100, 160 and 250 micron bands as well as by a photometric or spectroscopic redshift and 22-band photometry (GALEX, CFHT/Megacam, CFHT/WIRCam, AKARI, PACS and SPIRE channels). We also pay attention to discard any possible contamination from stars by carefully selecting each source according to their photometry and available spectroscopy.

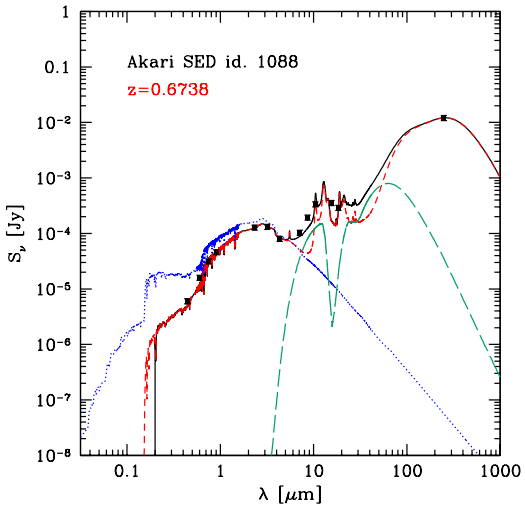

Figure 1. A typical SED fit obtained using the Berta et al. (2013) code showing the three components used to perform the fit: the stellar template (dotted line), the AGN component (long dashed line) and the starburst component (dashed line). The black solid line represents the total of the three components while the black solid squares are the observed photometry in each band.

3. THE SED FITTING PROCEDURES

In order to check the quality of our crossmatching procedure and to get the physical properties required in our

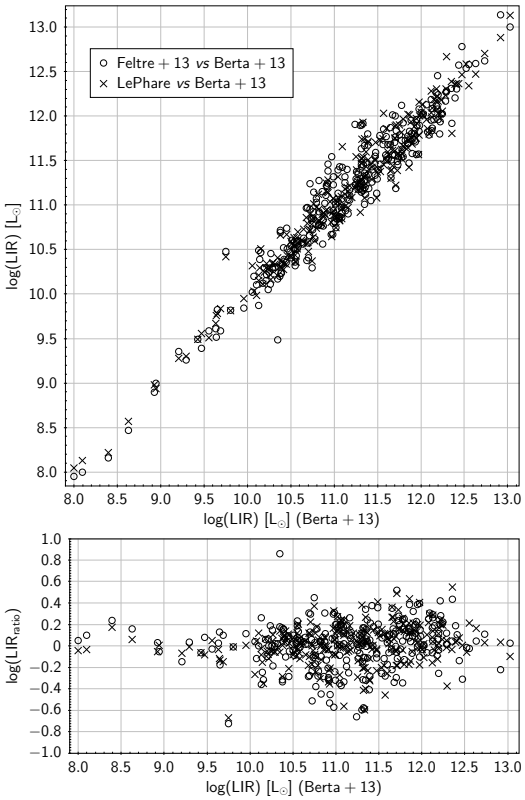

Figure 2. Top: Comparison between the rest-frame bolometric IR luminosity (8-1000 μm) obtained by different codes: `LePhare`, Feltre et al. (2013) and Berta et al. (2013); Bottom: Percentage difference between the rest-frame bolometric IR luminosity (8-1000 μm) obtained by `LePhare` or Feltre et al. (2013) procedures against estimates obtained using Berta et al. (2013) code (the symbols are reported in the same way as in the top panel).

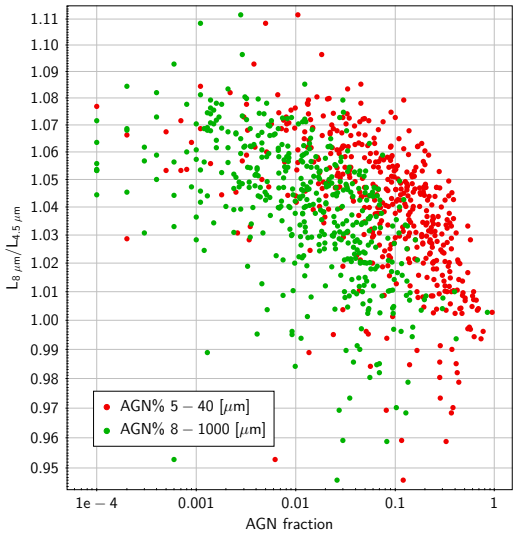

Figure 3. PAH luminosity ratio $\frac{L_{8\ \mu m}}{L_{4.5\ \mu m}}$ as a function of AGN fraction in different wavelength ranges.

study we proceed to fit the SEDs of our galaxies using different codes. We started using `LePhare` (Arnouts et al. 1999 and Ilbert at al. 2006) in 2 different modes. We fit the whole photometry in one go using a single set of template SEDs covering the whole spectrum from UV to FIR. In this way we checked that the positional cross-matching of the different catalogues did work and thus we verified that the photometry was consistent across the spectrum. To progress further we used the set of templates from Berta et al. (2013). Once we checked that the photometry was homogeneous across the spectrum, we proceeded with more sophisticated SEDs fitting procedures. We firstly used `LePhare` again but this time with a double set of templates according to the wavelength regime: in the Optical-MIR range (up to 8 μm) we use the same templates and extinction laws exploited by the COSMOS team to estimate the COSMOS photometric redshifts as in Ilbert et al. (2009) while to fit the IR-Submm range (from 8 μm upwards) we use the set of templates by Berta et al. (2013). This is straightforward procedure which gives us a first estimate of the SFR of our objects derived by the integration between 8 and 1000 μm of the FIR emission converted into SFR following Kennicutt (1998). We then exploited two codes optimised to determine the AGN properties by the SED analysis and which are able to give us more physical properties of our galaxies (e.g., stellar masses). The first one is the modified version of `Magphys` (da Cunha et al. 2008) implemented and used by Berta et al. (2013). The `Magphys` code is a powerful software to fit the SED of galaxies: it is user friendly, easily modifiable, covers the whole spectrum and it implements a self-consistent energy balance between the amount of energy absorbed by dust in the short-wavelength regime and dust emission at longer wavelengths. The approach implemented by Berta et al. (2013) differs from the original `Magphys` in several details, in particular, while the original version of the code considers that the light produced by the stars is the most significant source of dust heating, the approach implemented in Berta et al. (2013) adds a component of warm dust which represent the dust surrounding the AGN distributed as a torus around the active nucleus. This last step has been obtained by combining the da Cunha et al. (2008) code with the Fritz et al. (2006) AGN torus library. For more details on the code we refer the reader to Berta et al. (2013). The second procedure we used is the one developed by Fritz et al. (2006) and Feltre et al. (2012). This software is able, as in the previous case, to fit automatically a multi-component SED over the full spectral regime from the UV to the FIR. The code uses three energetic sources

of emission: a series of stellar population models (SSP) to reproduce the stellar UV/optical emission, a revised version of the Fritz et al. (2006) AGN torus models from Feltre et al. (2012) for the mid-IR emission and classical empirical starburst templates to reproduce the FIR peak of the SED. For more details on this code we refer the reader to Feltre et al. (2013). Using our SED fitting analysis we estimated the rest-frame luminosities in each band, the rest frame bolometric IR luminosity (8-1000 μm), the SFR and, from the last two codes, we also obtained physical quantities such as M_* and AGN related quantities such as AGN fraction and integrated luminosities. In particular we estimated the AGN fraction in four wavelength ranges: 5-40 μm, 10-20 μm, 20-40 μm and 8-1000 μm. This careful analysis will allow us to better discriminate between starburst dominated objects and AGN dominated objects and how they differ in their SFRs. In Figure 1 we present an example of the multi-component fit obtained using Berta et al. (2013) code.

4. RESULTS

Since any SED fitting procedure makes a number of assumptions in order to fit the observed photometry, comparing the results from different procedures applied to the same sample can give us more confidence in our results, allowing us to assess any possible bias generated by each procedure. For this reason, in this Section we report some preliminary comparisons between the results obtained from the various SED fitting codes described in Section 3 to investigate whether or not we have evidence of any code-related bias in our analysis. By integrating the total SED between 8-1000 μm we obtained estimates of the rest-frame bolometric IR luminosity which is commonly used as a tracer of the SFR in galaxies (Kennicutt 1998 assuming a Salpeter IMF: SFR $= k(\lambda)\mathrm{L}(\lambda)$ where $\mathrm{k(IR)} = 4.5 \times 10^{-44} \left[\frac{\mathrm{M_\odot yr^{-1}}}{\mathrm{ergs^{-1}Hz^{-1}}}\right]$). In Figure 2 we report the comparison of these estimates obtained by different procedures. All the adopted SED fitting procedures give broadly similar IR bolometric luminosities and thus similar SFRs. Similar results are obtained if we compare the M_* estimates, both Berta et al. (2013) and Feltre et al. (2013) methods in fact give similar M_* and IR bolometric luminosities estimates within the uncertainties ($\sim$ 20%). While a more conclusive analysis of how the presence of AGN affects the SFR of IR galaxies will be reported in Marchetti et al. in prep., here we present some preliminary analysis related to this topic. In Figure 3 we show how the ratio $\frac{L_{8\ \mu\mathrm{m}}}{L_{4.5\ \mu\mathrm{m}}}$ varies according to the AGN fraction as a function of wavelength ranges. We estimated the AGN fraction in 4 different rest-frame wavelength ranges (5-40 μm, 10-20 μm, 20-40 μm and 8-1000 μm) by integrating the best fit SEDs in these ranges and estimating the ratio between the energy emission given by the Torus component and the total energy distribution. This plot shows that the $\frac{L_{8\ \mu\mathrm{m}}}{L_{4.5\ \mu\mathrm{m}}}$ ratio decreases with increasing AGN fraction. The $L_{8\ \mu\mathrm{m}}$ is connected with the polycyclic aromatic hydrocarbon (PAH) emission. PAHs are believed to reside in photo-dissociation regions which are exited by the UV light emitted by stars and that re-emit their energy at very specific wavelengths: 3.3, 6.2, 7.7, 8.6 and 11.3 μm. Given this connection between the PAH luminosity and the absorbed light emitted by young stars, PAHs are commonly used as SFR tracers. In particular, among all the PAHs emission lines, the 7.7 μm is the strongest and dominates the luminosity at 8μm. It has also been shown that the $L_{8\ \mu\mathrm{m}}$ correlates strongly with the IR bolometric luminosity (Caputi et al. 2007) which, as we already said, traces the SFR in dust-obscured galaxies. For this reason, while studying how the AGN contribution may influence the total SFR estimates for galaxies, it is important to investigate how the PAH luminosity may change as a function of the AGN fraction. In Figure 3 we show that the ratio $\frac{L_{8\ \mu\mathrm{m}}}{L_{4.5\ \mu\mathrm{m}}}$, which can be used as a tracer of PAH deficit in galaxies (e.g., Murata et al. 2014) decreases with increasing AGN fraction, but that the AGN fraction contribution varies according to the wavelength range in which this contribution is estimated. For example, for the same value of $\frac{L_{8\ \mu\mathrm{m}}}{L_{4.5\ \mu\mathrm{m}}}$, we find that the AGN fraction is lower if we consider the range 8-1000 μm instead of the 5-40 μm range. This means that whenever we are looking at the AGN contribution and how this affects the SFR estimates, or whenever we try and separate starburst-dominated objects from AGN-dominated ones using the AGN fraction, we should be very careful in which wavelength range we are estimating such AGN fraction as our conclusions are deeply linked to this measurement.

5. SUMMARY & FUTURE PERSPECTIVES

We have analysed 1133 sources detected by AKARI, Herschel and by various multi-wavelength surveys at shorter wavelengths (22 photometric bands in total, from the UV to 500 μm). Thanks to this wavelength coverage we were able to study the overall properties of the SEDs of these objects in detail and in particular

the regime between 2 and 24 μm where the AGN emission contributes the most to the SED. The main aim of this work (which will be further developed in Marchetti et al., in prep.) is to contribute to the open debate about how AGN may influence the total SFR estimates of galaxies and change their distribution with respect to the *Galaxy Main Sequence*. This is of particular interest now that Herschel allows us to study the peak of the IR emission of galaxies, and thus the SFR, up to high redshift, along with the possible interplay between mergers and/or AGN feedback in the star formation of IR luminous galaxies. We applied three SED fitting procedures to get the M_*, the rest-frame luminosities in different bands, the infrared bolometric luminosity between 8-1000 μm and the SFR, and found that the three methods provide consistent estimates. In particular we applied two SED fitting procedures optimised to study the AGN emission from the SED (Feltre et al. 2013 and Berta et al. 2013) and we have estimated the AGN contribution to the total luminosity in 4 wavelength ranges. We have shown that $\frac{L_{8\ \mu\mathrm{m}}}{L_{4.5\ \mu\mathrm{m}}}$, which is related to the PAH emission in the galaxies, decreases with increasing AGN fraction but that this fraction changes if we estimate the AGN fraction in different wavelength ranges. In Marchetti et al. (in preparation) we will investigate in more detail the specific star formation rate (SSFR) of these objects and how this estimate may be affected by the presence of an AGN.

ACKNOWLEDGMENTS

LM and SS acknowledges support from the Science and Technology Facilities Council under grant ST/J001597/1. MV acknowledges support from the Square Kilometre Array South Africa project and from the South African National Research Foundation.

REFERENCES

Arnouts, S., et al., 1999, Measuring and modelling the redshift evolution of clustering: the Hubble Deep Field North, MNRAS, 310, 540

Berta, S., Lutz, D., Santini, P., et al., 2013, Panchromatic spectral energy distributions of Herschel sources, A&A, 551, A100

Brusa, M., Bongiorno, A., Cresci, G., et al., 2014, X-shooter reveals powerful outflows in $z \sim 1.5$ X-ray selected obscured quasi stellar objects, arXiv:1409.1615

Bower, R. G., Benson, A. J., Malbon, R., et al., 2006, Breaking the hierarchy of galaxy formation, MNRAS, 370, 645

Caputi, K. I., Lagache, G., Yan, L., et al., 2007, The Infrared Luminosity Function of Galaxies at Redshifts z = 1 and $z \sim 2$ in the GOODS Fields, ApJ, 660, 97

da Cunha, E., Charlot, S., & Elbaz, D., 2008, A simple model to interpret the ultraviolet, optical and infrared emission from galaxies, MNRAS, 388, 1595

Delvecchio, I., Gruppioni, C., Pozzi, F., et al., 2014, Tracing the cosmic growth of supermassive black holes to $z \sim 3$ with Herschel, MNRAS, 439, 2736

Elbaz, D., Dickinson, M., Hwang, H. S., et al., 2011, GOODS-Herschel: an infrared main sequence for star-forming galaxies, A&A, 533, A119

Farrah, D., Afonso, J., Efstathiou, A., et al., 2003, Starburst and AGN activity in ultraluminous infrared galaxies, MNRAS, 343, 585

Feltre, A., Hatziminaoglou, E., Fritz, J., & Franceschini, A., 2012, Smooth and clumpy dust distributions in AGN: a direct comparison of two commonly explored infrared emission models, MNRAS, 426, 120

Feltre, A., Hatziminaoglou, E., Hernán-Caballero, A., et al., 2013, The roles of star formation and AGN activity of IRS sources in the HerMES fields, MNRAS, 434, 2426

Fritz, J., Franceschini, A., & Hatziminaoglou, E., 2006, Revisiting the infrared spectra of active galactic nuclei with a new torus emission model, MNRAS, 366, 767

Kennicutt, R. C., Jr., 1998, The Global Schmidt Law in Star-forming Galaxies, ApJ, 498, 541

Kim, S. J., Lee, H. M., Matsuhara, H., et al., 2012, The North Ecliptic Pole Wide survey of AKARI: a near- and mid-infrared source catalog, A&A, 548, A29

Ilbert, O., et al., 2006, Accurate photometric redshifts for the CFHT legacy survey calibrated using the VIMOS VLT deep survey, A&A, 457, 841

Ilbert, O., Capak, P., Salvato, M., et al., 2009, Cosmos Photometric Redshifts with 30-Bands for 2-deg^2, ApJ, 690, 1236

Murakami, H., Baba, H., Barthel, P., et al., 2007, The Infrared Astronomical Mission AKARI, ASJ, 59, 369

Murata, K., Matsuhara, H., Wada, T., et al., 2013, AKARI North Ecliptic Pole Deep Survey. Revision of the catalogue via a new image analysis, A&A, 559, A132

Murata, K., Matsuhara, H., Inami, H., et al., 2014, Polycyclic aromatic hydrocarbon feature deficit of starburst galaxies in the AKARI North Ecliptic Pole Deep field, A&A, 566, A136

Oi, N., Matsuhara, H., Murata, K., et al., 2014, Optical - near-infrared catalog for the AKARI north ecliptic pole Deep field, A&A, 566, A60

Pilbratt, G. L., Riedinger, J. R., Passvogel, T., et al., 2010, Herschel Space Observatory. An ESA facility for far-

infrared and submillimetre astronomy, A&A, 518, L1

Rodighiero, G., Daddi, E., Baronchelli, I., et al., 2011, The Lesser Role of Starbursts in Star Formation at $z = 2$, ApJ, 739, L40

Rodighiero, G., Renzini, A., Daddi, E., et al., 2014, A multiwavelength consensus on the main sequence of star-forming galaxies at $z \sim 2$, MNRAS, 443, 19

Shim, H., Im, M., Ko, J., et al., 2013, Hectospec and Hydra Spectra of Infrared Luminous Sources in the AKARI North Ecliptic Pole Survey Field, ApJs, 207, 37

Werner, M. W., Roellig, T. L., Low, F. J., et al., 2004, The Spitzer Space Telescope Mission, ApJ, 154, 1